Hydrogen adsorption on the (100) surfaces of rhodium and palladium: the influence of non-local exchange - correlation interactions

1996 J. Phys.: Condens. Matter 8 7659

(http://iopscience.iop.org/0953-8984/8/41/012)

J. Phys.: Condens. Matter **8** (1996) 7659–7675. Printed in the UK

Hydrogen adsorption on the (100) surfaces of rhodium and palladium: the influence of non-local exchange–correlation interactions

A Eichler, J Hafner and G Kresse

Institut für Theoretische Physik and Centre for Computational Materials Science, Technische Universität Wien, Wiedner Hauptstraße 8-10/136, A-1040 Wien, Austria

Received 18 June 1996

Abstract. We report *ab initio* investigations of the adsorption of atomic hydrogen on the (100) surfaces of Rh and Pd in the local-density-functional and generalized-gradient approximations. Our calculations have been performed using a plane-wave basis, using optimized ultrasoft pseudopotentials for describing the electron–ion interactions. Detailed results are reported for the adsorption energies, the stabilities of various adsorption geometries, and the adsorption-induced changes in the surface relaxations and in the work-functions. We find that the adsorption of a monolayer of hydrogen changes the inward relaxation of the top layer of the substrate into an outward relaxation. However, the change of the substrate relaxation has only a very small influence on the adsorption energy and geometry. For both metals the stable adsorption sites are the fourfold hollows. The site preference has its origin in a maximum gain of covalent bonding energy resulting from the overlap of the hydrogen s and the metal $d_{x^2-y^2}$ orbitals and from a minimal Pauli repulsion. Non-local exchange–correlation corrections have only a small influence on the atomic adsorption process and on the relaxation of the substrate, but influence the adsorption energy through corrections to the binding energy of the hydrogen molecule. Relativistic effects, however, turn out to be quite important.

1. Introduction

The dissociation of small molecules and the adsorption of the dissociation products on transition-metal surfaces represent important steps in many catalytic reactions [1, 2]. In particular, the adsorption of atomic and the dissociative adsorption of molecular hydrogen represent prototype reactions that have been studied very thoroughly, both experimentally and theoretically. Recently it has been shown that quantitative predictions of adsorption energies and geometries might be possible on the basis of total-energy calculations within the framework of the local-density-functional approximation (LDA) [3–9]. Despite the undisputed success of the LDA, certain problems remain. (i) Due to the rapid variation of the electron density at the surface, it is clear that the description of the adsorbate–substrate interaction goes to the very limit of the applicability of the LDA. For the dissociative adsorption of a molecule in particular it has been shown that qualitatively different answers (e.g. presence/absence of a barrier in the reaction channel) are obtained using the LDA and using non-local corrections described in the generalized-gradient approximation (GGA) [10–12]. It is still unclear whether the non-local corrections affect also the predictions concerning the atomic adsorption, and in particular the adsorbate-induced modification of the substrate. (ii) Even today, a complete relaxation of the adsorbate/substrate complex

0953-8984/96/417659+17$19.50

remains a formidable computational task. Conventional total-energy calculations based on full-potential all-electron techniques consider at most a relaxation of the first surface layer [5–9] or deal simply with a bulk-terminated surface [10–12]. Here it appears to be advantageous to use plane-wave-based techniques that allow a straightforward calculation of the forces acting on the atoms and the stresses on the surface cells [13–15]. However, it is well known that plane-wave-based techniques are difficult to apply to transition and first-row elements.

In this work we present *ab initio* total-energy investigations of the adsorption of atomic hydrogen on the (100) surfaces of Rh and Pd within the local-density approximation, allowing for a full relaxation of the substrate and considering the possible influence of non-local and spin-polarization corrections to the exchange–correlation functional. Our calculations are performed in a plane-wave basis and using optimized ultrasoft pseudopotentials [16–18] for describing the electron–ion interaction for both the transition-metal atoms of the substrate and the adsorbed hydrogen atoms. The solution of the generalized Kohn–Sham equations is performed via efficient residual-minimization techniques [19–21]; the exact Hellmann–Feynman forces are used for the optimization of the adsorbate/substrate geometry.

Pd and Rh are case studies of particular interest. Pure Pd(100) surfaces show only minimal surface relaxation (-0.6% inward relaxation of the surface layer), in agreement with the LDA predictions [7–9]. On adsorption of a monolayer of hydrogen the outward relaxation of the top layer is predicted to increase to 5.2% [9]. For clean Rh(100) surfaces LDA calculations [3–7, 22] predict inward relaxations between -3.5 and -5.1%. Experimentally, the situation is less clear: for the relatively open (100) and (110) surfaces of Rh, LEED studies [23–28] also show inward relaxations, but there are large quantitative differences between the results of different groups. Still, for the Rh(100) surface in particular the conclusion seems to be that there is either no relaxation or only a small inward relaxation of $-1.2 \pm 1.6\%$ [29]. All-electron LDA calculations show that on adsorption of a monolayer of H the inward relaxation is either strongly reduced (from -5.1 to -1.4%, full-potential linearized-augmented-plane-wave (FLAPW) calculations [3, 4]) or changed to an outward relaxation (from -3.5 to $+1.1\%$, full-potential linearized-muffin-tin-orbital (FLMTO) calculations [8, 9]). However, the conclusion that the failure of the older LEED studies to find an inward relaxation was due to a contamination of the surface was contested by more recent experiments [29]. For Rh the situation has been further complicated by claims that the free surfaces are ferromagnetic [30] and that the surface magnetism strongly reduces relaxation. The predictions of surface magnetization were based on pseudopotential calculations without corrections for the non-linearity of the exchange–correlation functional. The ferromagnetism of Rh surfaces has been contested by both all-electron FLAPW calculations [31] and by pseudopotential calculations [32] predicting non-magnetic surfaces. Spin-polarized photoemission experiments [33] put an upper limit of 0.1 to 0.2 μ_B to the surface magnetic moment. The present paper concentrates on the possible influence of the non-locality of the exchange–correlation potential on the surface relaxation and on the microscopic explanation of the local surface reactivity.

2. Method

Our calculations have been performed using the Vienna *ab initio* simulation program (VASP) [19–21]. VASP is based on the following principles.

(1) We use the finite-temperature version of LDF theory [34] developed by Mermin [35],

with the exchange–correlation functional given by Ceperley and Alder as parametrized by Perdew and Zunger [36]. Finite-temperature LDF theory introduces a smearing of the one-electron levels and helps to solve convergence problems arising from using a small set of $\boldsymbol{k}$-points for Brillouin zone integrations. The use of fractional occupancies eliminates all instabilities that can arise from a crossing of levels in the vicinity of the Fermi energy.

(2) Non-local exchange–correlation effects are considered in the form of generalized-gradient corrections (GGCs). We used both the Perdew–Becke (see [37]) and Perdew–Wang (see [38]) GGC functionals.

(3) To investigate a possible magnetic polarization of the surface, spin-polarized calculations using the local-spin-density (LSD) functional of von Barth and Hedin [39] have been performed. For a correct treatment of spin polarization it is essential to account for the non-linearity of the LSD functional by incorporating partial core corrections [40].

(4) The solution of the generalized Kohn–Sham equations (using either the scalar-relativistic or the non-relativistic Hamiltonian) is performed using an efficient matrix-diagonalization routine based on a sequential band-by-band residual-minimization method (RMM) for the one-electron energies [21, 41].

(5) In the doubly iterative RMM method it is essential to use an efficient charge-density-mixing routine to avoid charge-sloshing problems. We use an improved Pulay mixing for calculating the new charge density and potential [42]. We have found that especially for metals the sequential band-by-band algorithm combined with an efficient mixing algorithm is considerably faster than conjugate-gradient (CG) algorithms for attempting a direct minimization of the energy by treating all bands simultaneously [21].

(6) The optimization of the atomic geometry is performed via a conjugate-gradient minimization of the total energy with respect to the atomic coordinates.

(7) After moving the atoms, the change in the charge density is estimated from the displaced atomic charge densities.

(8) The calculation has been performed using fully non-local optimized ultrasoft pseudopotentials [16–18]—this is very important for making calculations for large supercells tractable for transition metals.

For all further technical aspects we refer to the recent paper by Kresse and Furthmüller [21].

Table 1. Parameters determining the ultrasoft pseudopotentials for Rh, Pd and H: cut-off radii $R_{c,l}$, augmentation radii $R_{aug,l}$, and truncation radii R_{loc} for the local part of the potential (in Å).

	Rh	Pd	H
$R_{c,s}$	1.25	1.28	0.66
$R_{c,p}$	1.40	1.43	0.66
$R_{c,d}$	1.40	1.43	
$R_{aug,s}$	1.25	1.28	0.42
$R_{aug,p}$	1.25	1.28	
$R_{aug,d}$	1.14	1.16	
R_{loc}	0.97	0.99	

The parameters specifying the optimized ultrasoft pseudopotentials for Rh and Pd are given in table 1. The atomic reference states are $5s^1 4d^8$ (Rh) and $5s^1 4d^9$ (Pd). All of the angular-momentum components of the potential are described by ultrasoft pseudo-

Table 2. Atomic volume Ω, lattice constant a_0, cohesive energy E_0 and bulk modulus B for fcc Rh, calculated in the LDA and LDA + GGC approximations

	Ω (Å^3)	a_0 (Å)	E_0 (eV)	B (Mbar)
LDA, scalar-relativistic	13.396	3.770	−8.57	3.03
LDA + GGC(PB), scalar-relativistic	14.300	3.853	−6.99	2.48
LDA + GGC(PW), scalar-relativistic	14.255	3.849	−7.16	2.44
LDA, non-relativistic	13.740	3.802	−7.84	2.74
Experiment[a]	13.755	3.803	−5.75	2.69

[a] References [47–49].

potentials with two reference energies. One reference energy is always the eigenvalue of the reference configuration; the second is chosen such as to span the expected bandwidth. The precise location has little influence on the potential. The local potential is the all-electron potential truncated for radii smaller than R_{loc}. If non-local corrections to the exchange–correlation potentials are used for the bulk and surface calculations, they are also applied in the generation of the pseudopotential. Hydrogen is also described by an ultrasoft pseudopotential for the s component and a norm-conserving potential for the p component (see table 1). For the H_2 dimer the pseudopotential leads to good agreement of the calculated bond length, binding energy, and vibrational eigenfrequency of $d = 0.765$ Å, $E_B = 4.84$ eV, and $\omega = 4210$ cm^{-1} with the corresponding experimental values of $d = 0.74$ Å, $E_B = 4.75$ eV, and $\omega = 4395$ cm^{-1}. For all three pseudopotentials convergence with respect to the plane-wave basis set is achieved with a cut-off energy of $E_{cut} = 200$ eV.

3. Results

3.1. Bulk Rh and the clean Rh(100) surface

Table 2 lists the properties of bulk Rh calculated in the LDA and using the gradient-corrected exchange–correlation functionals proposed by Perdew and Becke (PB) [37, 43] and Perdew and Wang (PW) (see [38, 44]). We find that compared to the LDA the GGCs lead to an increase of the lattice constant and therefore also to a decrease of the bulk modulus. Since the overbinding of the LDA is rather small for the 4d metals, the GGCs tend to overcorrect the lattice constant. For the bulk modulus, the LDA value is considerably larger than the experimental one, so the GGCs lead to somewhat better agreement with experiment. As in our previous studies of the B-group elements [45, 46], we find that the effect of the gradient corrections is essentially to add an isotropic pressure favouring a slight expansion of the lattice. At a fixed volume, the GGCs change neither the structural energy differences nor the band-structure in any significant way.

Although total-energy calculations for the 4d elements are often performed non-relativistically, relativistic corrections can be quite essential. We find that a non-relativistic LDA calculation predicts an equilibrium lattice constant of $a = 3.802$ Å in almost perfect agreement with experiment and about 0.85% larger than the scalar-relativistic LDA result (cf. table 2). We shall see that even this small relativistic effect has a non-negligible effect on the energetics of an adsorbate.

For the adsorption calculations, the surfaces have been modelled by symmetric eight-layer slabs, fixing the two innermost layers at the coordinates of the bulk and relaxing the interlayer distances between the top three layers on each side. A (1×1) surface cell with one

Table 3. Relaxation of the clean Rh(100) surface (the changes Δd_{ij} of the interlayer distances as percentages of the distances in the bulk), calculated in the LDA and using Perdew–Becke (PB) and Perdew–Wang (PW) gradient corrections.

		LDA[a]	PB[a]	PW[a]	US-PP[b]	LMTO[c]	LAPW[d]
Δd_{12}	(%)	−3.2	−2.8	−3.9	−3.8	−3.5	−5.1
Δd_{23}	(%)	0.7	0.4	0.0	0.7		
Δd_{34}	(%)	0.7	0.0	−0.2	0.6		

[a] Present work.
[b] Using the same pseudopotentials, but thicker slabs; reference [22].
[c] Reference [4], LDA.
[d] Reference [7], LDA.

atom per cell has been used, Brillouin zone integrations have been performed using grids of $(11 \times 11 \times 1)$ Monkhorst–Pack [50] special points and the Methfessel–Paxton technique [51] for a generalized Gaussian smearing of the one-electron eigenstates. The optimization of the surface geometry has been performed using a static conjugate-gradient minimization using the Hellmann–Feynman forces. All surface calculations are always performed at the equilibrium lattice constant of the bulk.

Within the LDA we calculate within this setting an inward relaxation of the top layer by $\Delta_{12} = -3.2\%$ and slight outward relaxations of the next two layers (see table 3), in reasonable agreement with our earlier calculations using thicker layers in a (1×1) geometry [22] and with earlier all-electron calculations restricting the relaxation to the top layer only [4, 7]. Introduction of the non-local corrections to the exchange–correlation functional leads only to marginal changes: using the PB-GGC functional Δ_{12} is reduced to -2.8%; with the probably more accurate PW-GCC functional it increases to $\Delta_{12} = -3.9\%$. In both cases the relaxation of the subsurface layers is slightly weaker than in the LDA (see table 3). Altogether we can conclude that gradient corrections do not modify the LDA predictions concerning surface relaxation in any significant way.

We have also investigated the possibility of the formation of a ferromagnetic surface layer. However, in contradiction to Morrison *et al* [30] and in agreement with Weinert and Blügel (see [31]) and Cho and Kang [32] we find that the Rh(100) surface is non-magnetic. Even if the calculations are initialized with a surface moment as large as that claimed by Morrison *et al*, the converged solution is always paramagnetic. Hence even a metamagnetic state of the surface seems to be excluded.

3.2. Hydrogen adsorption on Rh(100)

3.2.1. Geometry and energetics. To determine the stable adsorption geometry we have allowed, in addition to the relaxation of the substrate, a minimization of the total energy with respect to the height of the adsorbed hydrogen atom measured from the centre of the top layer of the substrate. Three different high-symmetry positions of the adsorbate (on top of a substrate atom, in a position forming a bridge between two nearest-neighbour surface atoms, and in the fourfold hollows in the (100) surface of the face-centred cubic crystal) have been considered. The binding energy as a function of the coverage θ (=number N_H of hydrogen atoms per metal atom in the top layer of the substrate) has been defined as the difference between the total energies of the hydrogen-covered surface $E_{M:H}$ and the clean

Table 4. Substrate relaxation Δ_{ij} (in per cent), binding energy E_b, adsorption energy E_{ad} (in eV, calculated using the experimental energies of the hydrogen atom or the molecule), height h_0 of the stable adsorption site above the surface layer (in Å), and work-function Φ (in eV) for H on different sites of the Rh(100) surface. Results calculated in the LDA and using the PB and PW gradient corrections are reported. For the LDA, the numbers in parentheses have been calculated with the substrate fixed in the geometry of the clean surface.

LDA				
		On top	Bridge	Hollow
Δ_{12}	(%)	−3.0	−1.6	0.4
Δ_{23}	(%)	1.3	0.5	−0.3
Δ_{34}	(%)	0.2	0.5	−0.7
h_0	(Å)	1.57(1.57)	1.14(1.15)	0.57(0.59)
E_b	(eV)	2.35(2.35)	2.75(2.75)	2.85(2.82)
E_{ad}	(eV)	−0.03(−0.03)	0.38(0.38)	0.48(0.45)
PB-GGC				
		On top	Bridge	Hollow
Δ_{12}	(%)	−3.1	−1.2	0.2
Δ_{23}	(%)	0.6	0.1	−1.2
Δ_{34}	(%)	−0.4	0.0	−0.2
h_0	(Å)	1.58	1.14	0.45
E_b	(eV)	2.47	2.84	2.85
E_{ad}	(eV)	0.10	0.47	0.48
PW-GGC				
		On top	Bridge	Hollow
Δ_{12}	(%)	−3.3	−1.5	0.5
Δ_{23}	(%)	0.6	0.1	−1.0
Δ_{34}	(%)	−0.4	0.1	0.1
h_0	(Å)	1.58	1.14	0.51
E_b	(eV)	2.42	2.78	2.82
E_{ad}	(eV)	0.05	0.41	0.45
Φ	(eV)	5.75	5.80	5.39

surface E_M plus the total energy of the appropriate number of free hydrogen atoms:

$$E_b(\theta) = -\frac{1}{N_H}[E_{M:H}(\theta) - E_M - N_H E_H].$$

The adsorption energy E_{ad} is defined as the energy difference between the hydrogen-covered surface and the clean surface plus $N_H/2$ hydrogen molecules:

$$E_{ad}(\theta) = -\frac{1}{N_H}\left[E_{M:H}(\theta) - E_M - \frac{N_H}{2}E_{H_2}\right]$$

i.e. the binding energy and adsorption energy differ by half of the binding energy of the H_2 molecule. When comparing the calculated binding and adsorption energies with experiment, we have to keep in mind that density-functional predictions are less accurate for atoms and molecules than for solids and surfaces. For the total energy of the H atom we have: $E_H(\mathrm{LDA}) = 12.132$ eV, $E_H(\mathrm{exp}) = 13.6058$ eV; and for the binding energy of the H_2 molecule: $E_{H_2}(\mathrm{LDA}) = 4.84$ eV, $E_{H_2}(\mathrm{exp}) = 4.75$ eV (according to reference [52]). To get a reasonable estimate of the stability/instability of an adsorption site unbiased by the inaccuracy of the atomic and molecular results it is therefore appropriate to use the experimental energies of the H atom and the H_2 molecule.

Table 4 summarizes our results for the hydrogen-covered Rh(100) surface. For all adsorption sites we have assumed a coverage of $\theta = 1$. In the LDA we find that the most stable adsorption site is $h_0 = 0.57$ Å above the fourfold hollow, allowing for a full relaxation of the substrate. For this geometry the adsorption energy is 0.1 eV/atom higher than in the bridge position where the equilibrium distance from the surface is $h_0 = 1.14$ Å. The effect of the adlayer is to weaken the back-bonding of the top Rh layer to the subsurface layer and to reduce the inward relaxation to $\Delta_{12} = -1.6\%$ in the bridge position and to turn it into a weak outward relaxation for H in the hollow. The on-top position is marginally instable against desorption of H_2 and leaves the geometry of the clean surface almost unchanged. It is remarkable that the relatively large adsorbate-induced changes of the substrate geometry have almost no influence on the energetics of the adsorption process: fixing the atoms of the substrate in the equilibrium positions in the clean substrate does not change the adsorption energies in the on-top and bridge positions at all and reduces that in the hollow position by merely 0.03 eV/atom.

Table 5. Comparison of the calculated binding energy E_b (in eV/atom) and height h_0 (in Å) of the adsorbed H atom, relaxation of the top layer Δ_{12} and work-function Φ (in eV) for Rh(100) (values refer to calculations in the GGA, with LDA results given in parentheses), compared with experiment and older calculations.

			Experiment[a,b]	Present work GGA-PW(LDA)	FLAPW[c] LDA	FLMTO[d] LDA	Green's function[e] LDA
Clean Rh(100)	Δ_{12}	(%)	???	−3.9(−3.2)	−5.1	−3.5	−3.1
	Φ	(eV)	5.11	5.15	5.50	5.25	
H:Rh(100)	E_b	(eV)		2.42(2.35)	1.98		
on top	h_0	(Å)		1.58(1.58)	1.64		
	Δ_{12}	(%)		−3.3(−3.0)			
	Φ	(eV)		5.75	5.81		
H:Rh(100)	E_b	(eV)		2.78(2.75)	2.50	2.62	2.64
bridge	h_0	(Å)		1.14(1.14)	1.19	1.15	1.12
	Δ_{12}	(%)		−1.5(−1.6)		−0.6	
	Φ	(eV)		5.80	5.89	5.74	
H:Rh(100)	E_b	(eV)	2.74	2.82(2.85)	2.67	2.78	2.76
hollow	h_0	(Å)		0.51(0.57)	0.58	0.38	0.65
	Δ_{12}	(%)		+0.5(+0.4)	> -1.4	1.1	
	Φ	(eV)	∼ 5.3	5.39	5.66	5.64	

[a] Reference [2].
[b] References [54–57].
[c] References [3, 4, 53].
[d] After references [7–9].
[e] After references [5, 6].

The influence of the GGCs on the adsorption properties is surprisingly weak. For the unstable adsorption sites the GGCs lead to an increase of the binding energies (calculated with the experimental total energy of the free H atom) by about 0.1 eV/atom for the PB and ∼0.05 eV/atom for the PW functional, i.e stabilizing the on-top site against desorption of H_2. The stable adsorption geometry is essentially unchanged—this concerns the position of the adsorbate as well as the relaxation of the substrate. For the stable adsorption site within the fourfold hollow, the inclusion of the GGCs leaves the adsorption energy almost unchanged (hence the energetic preference of the hollow over the bridge site is now very

small), but predicts that the adsorbate sinks somewhat deeper into the hollow (h_0 is reduced from 0.57 Å to 0.51 Å). The reduced energy difference for bridge-site against hollow-site adsorption is important since it suggests that higher than monolayer coverage might be achieved by putting H atoms on bridge sites.

In the GGC approximation only we have also calculated the work-function Φ for the clean and hydrogen-covered surfaces in terms of the difference between the selfconsistent potential (minus the exchange–correlation potential) in the vacuum and the Fermi level. For the clean surface we find a work-function of $\Phi = 5.15$ eV in excellent agreement with experiment [54]. Adsorption of a monolayer of H in the fourfold hollows increases Φ by 0.24 eV. A much more pronounced increase is predicted for the less stable adsorption sites. The variation of the work-function upon adsorption of hydrogen has been studied by Polizzotti and Ehrlich [55] and by Richter *et al* [57]. Both experiments lead to $\Delta\Phi \sim 0.2$ eV at an estimated coverage of one monolayer.

Table 6. Relativistic effects on the relative stability of the adsorption sites for H on Rh(100): the differences ΔE_b between the binding energies of the H atom in the hollow and bridge sites.

			Present work Scalar-relativistic	Present work Non-relativistic	FLMTO[a] Non-relativistic
Rh	ΔE_b	(eV)	0.10	0.21	0.16
Pd	ΔE_b	(eV)	0.19	0.31	0.32

[a] References [8, 9].

Comparison with earlier calculations and with experiment (see table 5) shows that our pseudopotential approach achieves reasonable agreement with all-electron calculations [3–6, 8, 9, 53]. The most important difference from the older calculations appears in the energy difference between bridge- and hollow-site adsorption, and in the height of the stable adsorbate position. We find that the diverging predictions for $\Delta E_b = E_b(\text{hollow}) - E_b(\text{bridge})$ can be attributed largely to the neglect of relativistic effects in the all-electron calculations. If we repeat our calculations with a non-relativistic Hamiltonian, we find that within the LDA ΔE_b increases from 0.1 eV/atom to 0.21 eV/atom, See table 6 (for simplicity the non-relativistic calculations have been performed with a fixed bulk-terminated geometry, but we have already shown that relaxation energies have only a small influence on the adsorption energies), recovering the agreement with the earlier all-electron calculations. However, the scalar-relativistic results should be considered as more accurate. This means that at least at higher temperatures, a simultaneous occupation of bridge and hollow sites cannot be excluded.

The predictions of the all-electron calculations for the height of the stable adsorption site show considerable scatter. We believe that the predictions based on the minimization of the total energy within a multidimensional (usually two-dimensional) parameter space are relatively inaccurate; calculation using the Hellmann–Feynman forces allows a more accurate prediction of the equilibrium geometry.

Differences also appear in the predictions for the change of the work-function on adsorption: we find $\Delta\Phi = 0.24$ eV for a monolayer of H in the fourfold hollows, the FLAPW calculations predict $\Delta\Phi = 0.16$ eV, the FLMTO calculations $\Delta\Phi = 0.39$ eV (both in the LDA). For this coverage, experiments show an increase of the work-function by $\Delta\Phi \sim 0.2$ eV [55, 57], in confirmation of the FLAPW and pseudopotential results, but in contradiction to the FLMTO data.

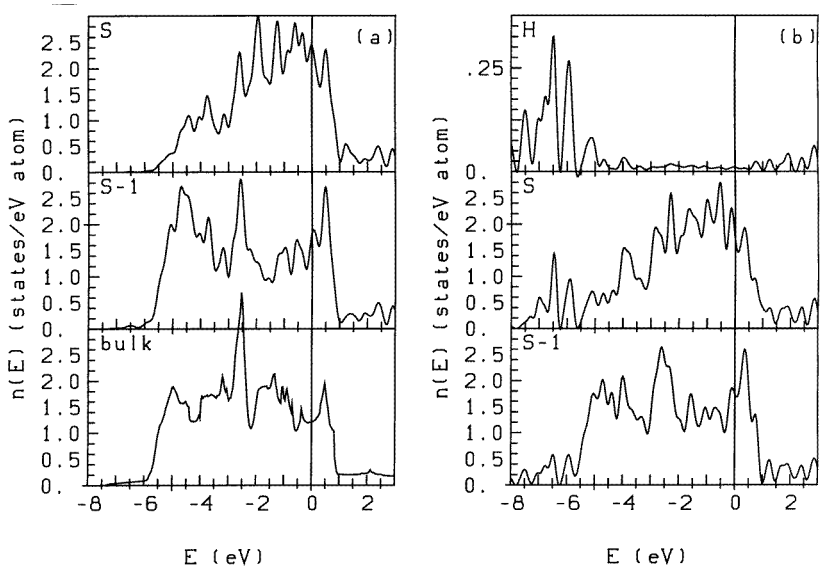

Figure 1. Local electron densities of states (a) in the surface and first subsurface layer of clean Rh(100), (b) in the adsorbed H layer and the first two Rh layers of H:Rh(100) (H atoms in the fourfold hollows), compared with the DOS in bulk Rh.

3.2.2. Surface electronic structure. Figure 1 shows the local electronic density of states in the adsorbed H layer (H atoms situated in the fourfold hollows) and in the surface and first subsurface Rh layers, compared with the local DOS of the clean Rh(100) surface and in the bulk. As already discussed in our previous paper [22], the characteristic feature of the DOS at the clean surface is the narrowing of the d band and the partial filling of the minima separating the three peaks in the bulk DOS that can be ascribed roughly to the bonding, non-bonding, and antibonding states. We refer to this paper for an in-depth discussion of the relationship between surface electronic structure and surface relaxation. For the stable adsorption geometry with the H atoms sitting in the fourfold hollows, H–Rh bonding states appear below the bottom of the d band for the clean Rh surface. These states are strongly localized in the top layer of the substrate and on the adsorbate atoms. The formation of the bonding H–Rh states at high binding energies is accompanied by a depletion of d states in the lower part of the d band.

A similar analysis with the H atom adsorbed in the less stable adsorption sites shows that there are quite pronounced variations of the binding energy of the adsorbate states: The lower the binding energy of the adsorbate, the lower the binding energy of the H–Rh surface states, as expected. However, in addition we find a pronounced variation of the form of the Rh d band in the surface layer which may be related to a preferred interaction of the H s states with Rh d states of different symmetry, depending on the adsorption site. These interactions evidently determine the local chemical reactivity.

At least at the relatively high coverage of a monolayer the H–Rh bonding states are not localized states, but they are delocalized over the entire surface plane and form a surface band well separated from the d states in the bulk projected onto the surface Brillouin zone. This is shown in figures 2(a) (surface band-structure) and 2(b) (charge density of the H–Rh surface states in a plane perpendicular to the surface and extending along the $\langle 110 \rangle$ direction).

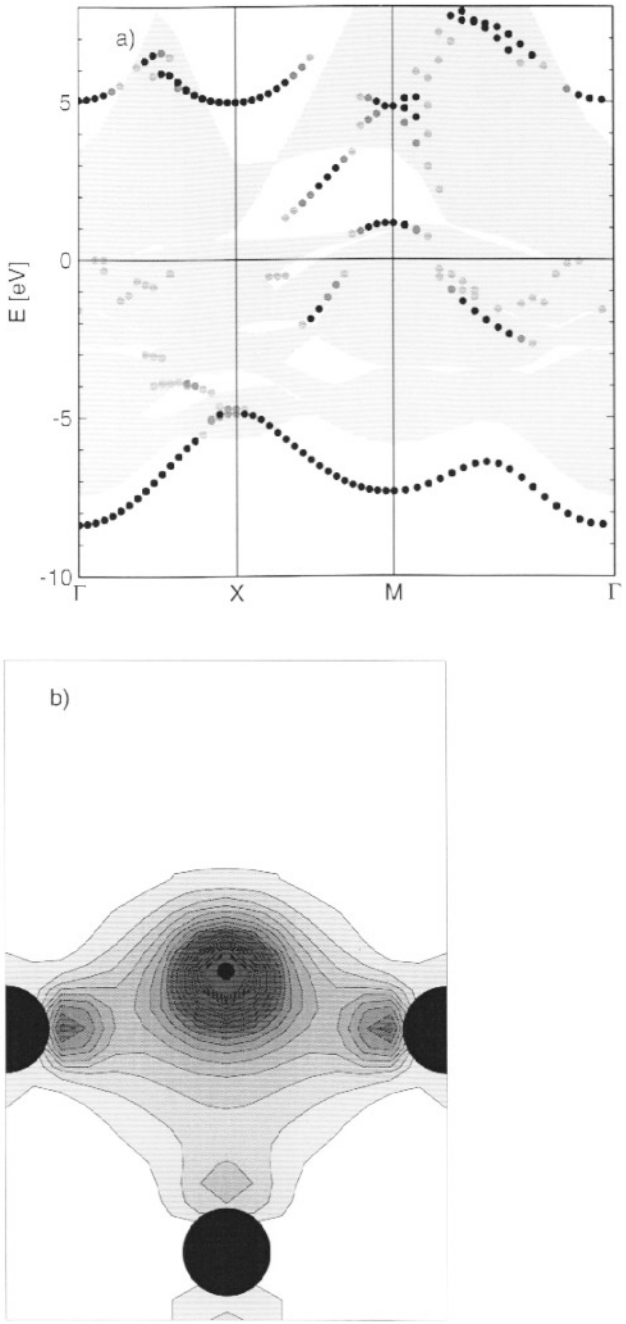

Figure 2. (a) Surface band-structure for H:Rh(100) with the H atoms adsorbed in the fourfold hollows. The shaded areas show the band-structure of the bulk projected onto the surface Brillouin zone; the full dots mark the dispersion relations of the surface band (different degrees of shading indicate the degree of localization: more than 85, 70 or 55% of the total intensity in the surface + adsorbate layers). The surface band-structure of the clean Rh(100) surface may be found in reference [22]. (b) A contour plot of the charge-density distribution corresponding to the states in the energy range of the H–Rh surface states (from −8 eV to −5 eV binding energy). Charge-density contours are drawn in the range between 0.01 to 0.2 electrons $Å^{-3}$, at intervals of 0.01 electrons.

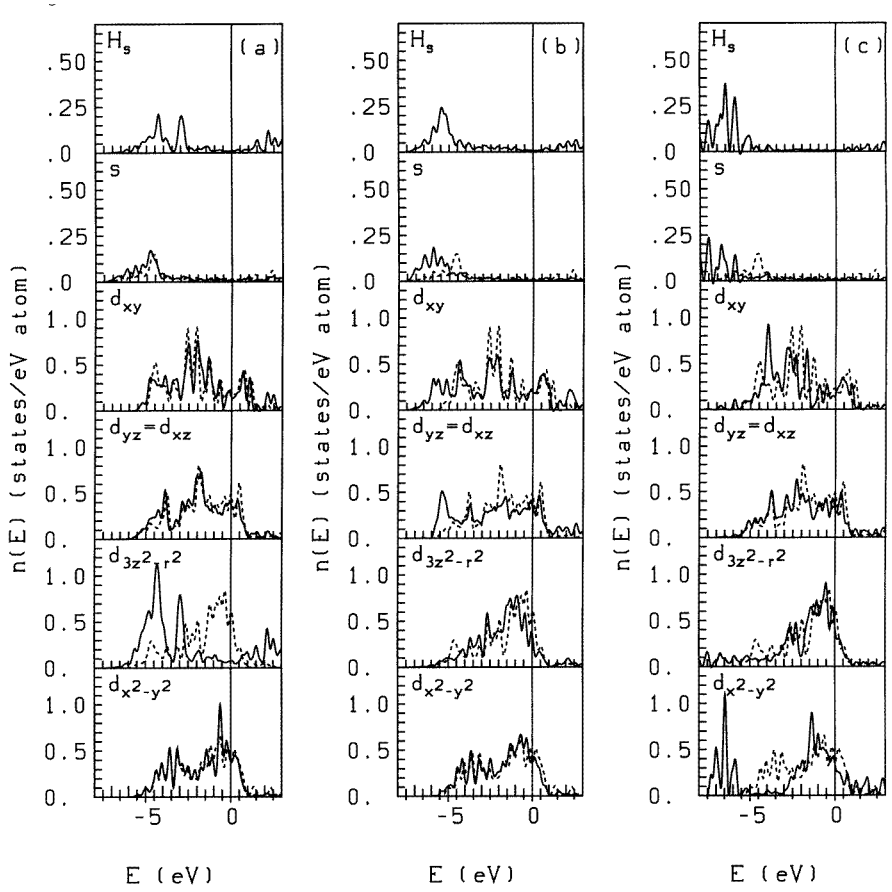

Figure 3. Partial local densities of states in the surface layer of the substrate and on the adsorbate sites for H:Rh(100) with the H atom in the on-top (a), bridge (b), and hollow (c) positions, respectively. The full lines show the local partial DOSs for the H-covered surface; the broken lines show for comparison the DOSs for the clean surface.

3.2.3. Local chemical reactivity. The preference for adsorption in the fourfold hollows on the (100) surfaces of fcc metals is usually attributed to two important factors: (i) the higher coordination (four against two for the bridge site), and (ii) minimization of the Pauli repulsion between the overlaping charge densities of the adsorbate and the substrate. On the other hand there have been many attempts to correlate the reactivity of a surface with simple properties such as the local surface DOS at the Fermi level $n_i(E_F)$ [58, 59] or the number of holes in the d band [60]. More general discussions suggest that these correlations are just a limiting case of a more general measure of the surface reactivity [61, 62]. Very recently Hammer and Norskov [63] have argued that $n_i(E_F)$ alone is not sufficient to differentiate between the surfaces of different metals and that quantitative analysis of the surface reactivity must be based on the hybridization of the metal d states with the orbitals of the adsorbate. Here we want to show that this hybridization is also a valid guideline for the selection of the most stable adsorbate site.

Figures 3(a)–3(c) show the partial local densities of state of the adsorbate and of the

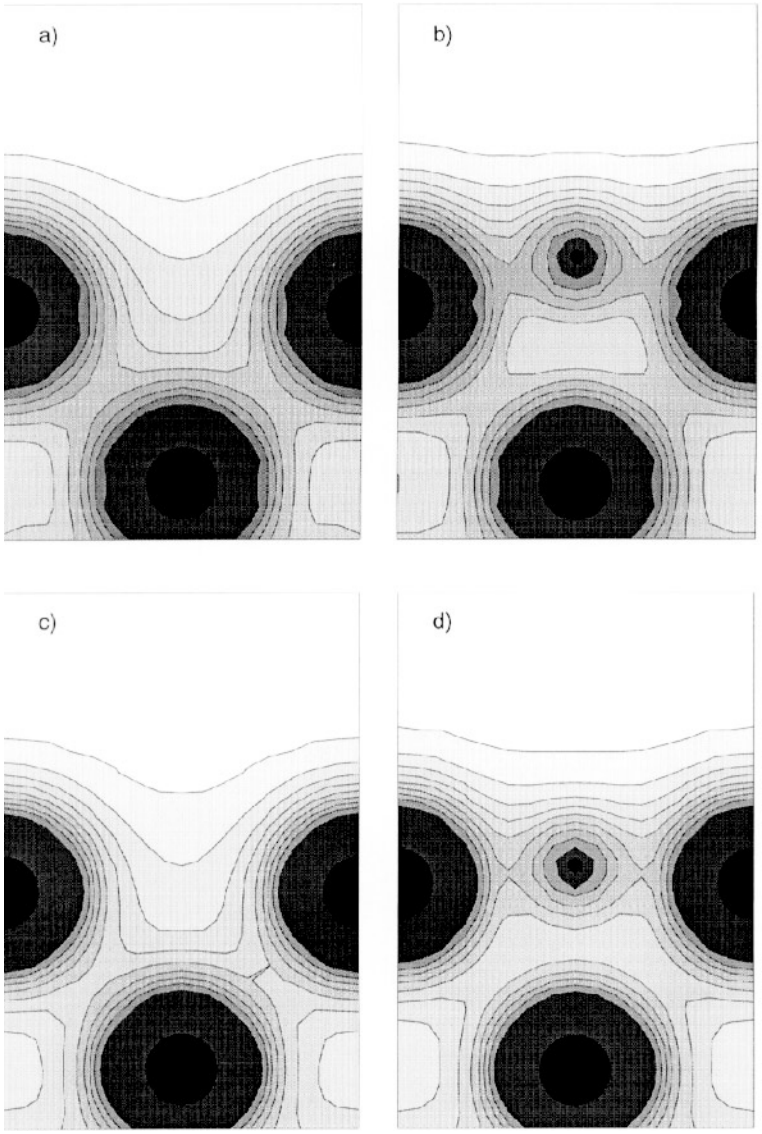

Figure 4. Contour plots of the electron density in a [011] plane perpendicular to the (100) surface of Rh ((a), (b)) and Pd ((c), (d)), without ((a), (c)) and with ((b), (d)) an adsorbed H atom. The equilibrium position of the H atom in the fourfold hole is marked by a black dot. Distances between constant-density contours follow a logarithmic scale between 0 and 1 electrons Å^{-3}.

first layer of the substrate, calculated for the clean surface and for H:Rh(100) with the adsorbed atom in the on-top, bridge, and hollow positions. In the on-top position, the strongest interaction occurs between the H s states and the Rh $d_{3z^2-r^2}$ states, i.e. with the d states having the largest spatial extent perpendicular to the surface. The centre of gravity of the bonding H s–Rh $d_{3z^2-r^2}$ states lies at a binding energy of about −4.5 eV; antibonding states appear about 2 eV above the Fermi level. The remaining orbitals of the substrate are hardly influenced by the H adsorption. If the H atom is placed at the bridge

Table 7. Atomic volume Ω, lattice constant a_0, cohesive energy E_0 and bulk modulus B for fcc Pd, calculated in the LDA and LDA + GGC approximations

	Ω (Å^3)	a_0 (Å)	E_0 (eV)	B (Mbar)
LDA, scalar-relativistic	14.324	3.855	−6.44	2.22
LDA + GGC(PW), scalar-relativistic	15.537	3.961	−5.20	1.56
LDA, non-relativistic	14.981	3.913	−6.04	1.99
Experiment[a]	14.686	3.887	−3.94	1.96

[a] References [47, 49, 68].

Table 8. Calculated binding energy E_b (in eV/atom), height h_0 (in Å) of the adsorbed H atom, relaxation of the substrate layers Δ_{ij}, and work-function Φ (in eV) for Pd(100), compared with experiment and older calculations.

			Experiment[a]	Present work GGA-PW	FLMTO[b] LDA	PP[c] LDA
Clean Pd(100)	Δ_{12}	(%)	∼ 0	−1.0	−0.6	
	Δ_{23}	(%)		+ 0.1		
	Δ_{34}	(%)		+ 0.1		
	Φ	(eV)	5.22	5.14	5.30	5.25
H:Pd(100)	Δ_{12}	(%)		+ 2.7		
on top	Δ_{23}	(%)		+ 1.1		
	Δ_{34}	(%)		−0.4		
	E_b	(eV)		2.21	2.20	1.86
	h_0	(Å)		1.55	1.56[d]	1.56
	Φ	(eV)		5.48	5.48	
H:Pd(100)	Δ_{12}	(%)		+ 1.9	+ 3.2	
bridge	Δ_{32}	(%)		+ 0.8		
	Δ_{34}	(%)		−0.8		
	E_b	(eV)		2.69	2.36	2.50
	h_0	(Å)		1.00	1.04	1.00
	Φ	(eV)		5.77	5.69	
H:Pd(100)	Δ_{12}	(%)		+ 4.4	+ 5.2	
hollow	Δ_{23}	(%)		+ 0.2		
	Δ_{34}	(%)		−0.8		
	E_b	(eV)	2.91	2.81	2.83	2.92
	h_0	(Å)	< 0.3	0.20	0.11	0.24
	Φ	(eV)	∼ 5.34	5.42	5.48	5.53

[a] After references [64–66].
[b] After references [7–9].
[c] After reference [67].
[d] The position of the H atom in the on-top position was not relaxed in FLMTO calculations.

site, the interaction is strongest with the d_{xy} orbitals of the substrate extending along the direction of the nearest-neighbour bonds in the surface plane, with bonding states centred at about −5.5 eV and antibonding states at energies >2 eV. For the H atom in the hollow, a very strong interaction with the Rh $d_{x^2-y^2}$ orbitals extending into the hollow leads to the formation of bonding states well below the bottom of the metal d band (centred at −6.5 eV) and antibonding states well above the Fermi level. The shift of the d states caused by the formation of the H–Rh bonds is proportional to the strength of the s–d transfer integral

and the coordination number. We conclude that the formation of covalent H s–metal d states is an important element in determining the site selectivity of H adsorption on (100) metal surfaces. A second important factor is to minimize the Pauli repulsion between the overlapping charge densities of the adsorbate and the substrate. Figure 4 shows the charge densities of the clean and hydrogen-covered Rh(100) surfaces in a plane passing through the surface normal and a nearest-neighbour bond in the surface. We find that the adsorbed atom fits perfectly into the charge-density minimum in the surface, while a sufficient overlap of the tails allowing the formation of covalent bonds is maintained.

3.3. Hydrogen on the Pd(100) surface

To show that the results found for H adsorption on Rh(100) are of general validity for fcc transition metals with a nearly full d band, we have briefly considered H adsorption on Pd(100). Table 7 summarizes the LDA and GGC results for the cohesive properties of bulk Pd. As for Rh we find that the generalized-gradient approximations overcorrect the characteristic LDA overbinding, with $\pm 1.7\%$ deviations for the equilibrium lattice constant. Again the less accurate non-relativistic calculations in the LDA agree somewhat better with experiment than the more accurate scalar-relativistic calculations.

Table 8 summarizes our results for the clean and H-covered Pd(100) surfaces. Only the results obtained using the GGC-PW functional are reported. For clean Pd(100) our calculations predict a -1.0% inward relaxation of the top layer, and a minimal outward relaxation of the next two layers. It is characteristic that we predict a slightly larger relaxation than that found in the FLMTO calculations [7] ($\Delta_{12} = -0.6\%$) where only the top layer has been allowed to relax. Both results agree with experiment within the experimental uncertainty. The adsorption energies are slightly smaller than at the Rh surface. The on-top site is again unstable against desorption of H_2. The stable adsorption site is again the fourfold hollow, with an adsorption energy about 0.12 eV larger than for the bridge site. The energetic preference of the hollow over the bridge site is larger than on Rh(100) ($\Delta E_b = 0.12$ eV for Pd(100) against $\Delta E_b = 0.04$ eV for Rh(100)), but again distinctly smaller than predicted in the non-relativistic all-electron (FLMTO) calculations of Wilke *et al* [8, 9] and in the pseudopotential calculations (with norm-conserving pseudopotentials) of Tomanek *et al* [67]. The difference from the present results stems again from relativistic effects: in non-relativistic calculations the difference between the binding energies increases to $\Delta E_b = 0.31$ eV, in reasonable agreement with the non-relativistic FLMTO and PP calculations.

Compared to the case for Rh(100), the height of the adsorbate above the surface is reduced for both the bridge and the hollow sites. For the latter site, h_0 is reduced from 0.51 Å to 0.20 Å. This is clearly a consequence of the larger lattice constant and the more localized 4d states of Pd, leading to a stronger corrugation of the electron-density profile at the surface (see figure 4) and to the formation of 'sinks' of low electron density admitting of the presence of an adsorbate atom at a minimal Pauli repulsion.

The H coverage leads to pronounced outward relaxation of the top layer of the substrate, by $\Delta_{12} = 2.5,\ 1.9,$ and 4.4% for the H atom in the on-top, bridge, and hollow sites, and also quite pronounced outward relaxations of the subsurface layers. This shows that the adsorption influences the metallic bonding quite deep into the substrate. In the all-electron calculation of Wilke *et al* [8, 9] where only top-layer relaxation has been considered, the outward relaxation is roughly equal to the sum of the relaxation of the surface and the subsurface layers in our calculation. The calculated work-function for the clean Pd surface is in good agreement with experiment [66] and with earlier calculations (see table 8

for details). The predicted change in the work-function induced by the adsorption of a monolayer of H of $\Delta\Phi = 0.28$ eV is nearly the same as that on Rh(100), in reasonable agreement with the FLMTO calculations ($\Delta\Phi \sim 0.18$ eV), but somewhat larger than found experimentally ($\Delta\Phi \sim 0.12$ eV according to [64]).

The electronic structure and the local chemical reactivity can again be analysed in the same manner as for the Rh surface, with largely equivalent results.

4. Conclusions

The conclusions to be drawn from this study concern (i) the computational problems associated with *ab initio* studies of transition-metal surfaces, (ii) the necessity to account for non-local corrections to the local exchange–correlation functional, and (iii) the physics and chemistry of the adsorption process.

Concerning (i), we have demonstrated that plane-wave-based pseudopotential techniques applied to transition-metal surfaces are as accurate as all-electron techniques. Using optimized ultrasoft pseudopotentials helps to reduce the size of the plane-wave basis set, the use of efficient iterative matrix diagonalization and charge-density-mixing techniques minimizing the number of orthogonalization operations [21] brings a further reduction of the computational effort. This allows to use larger and therefore more realistic slab models. The possibility of calculating the Hellmann–Feynman forces and stresses allows an unrestricted optimization of the geometry of the adsorbate/substrate complex.

(ii) Non-local exchange–correlation effects: for transition metals, the use of GGA corrections tends to overcorrect the LDA overbinding in the bulk. At the clean surface, the GGA leaves the surface relaxations calculated in the LDA almost unchanged. For the adsorption of atomic hydrogen the GGA leads to a marginal increase of the binding energy of H calculated at the equilibrium lattice parameter (mostly for the unstable adsorption sites, the changes for the stable site in the fourfold hollow are minimal), but no change in the adsorption geometry (adsorption height, adsorbate-induced change in the surface relaxation). In view of the rapid variation of the charge density normal to the surface, this result might seem to be quite surprising. The GGAs affect, however, the calculation of the adsorption energy via the corrections to the binding energy of the free H_2 molecule, in accordance with recent results on the dissociative adsorption of a diatomic molecule [10–12]. We also note briefly that the neglect of relativistic effects compensates a proportion of the LDA errors for the lattice constant and the binding energy in the bulk. However, neglect of relativistic effects can induce non-negligible errors in the structural predictions for the adsorbate.

(iii) For both Rh(100) and Pd(100), adsorption of atomic H occurs in the fourfold hollows. However, the energy difference with respect to adsorption on the bridge sites is rather small so that at higher coverage and higher temperatures, partial occupancy of the bridge sites has to be expected. The energy difference between the various adsorption sites was found to be quite sensitive to relativistic effects. For both metals, H adsorption induces pronounced changes in the surface relaxation: due to the hybridization of the H s states with the bonding metal d states at the bottom of the bands the metal–metal bonding is weakened in the surface layers, leading to an adsorbate-induced outward relaxation of the top layer relative to the clean relaxed surface. However, the binding energy and position of the adsorbate turn out to be relatively insensitive to the change in the relaxation, so for these quantities, a calculation based on the bulk-terminated surface seems to be justified. We have also demonstrated that the interaction between the H s states and the metal d states is strongly influenced by the adsorption geometry: binding in the fourfold hollows occurs through the formation of bonding H s–TM $d_{x^2-y^2}$ states, while a H atom placed in the top

position interacts mainly with the TM $d_{3z^2-r^2}$ states. However, in both cases the bonding states are formed at relatively high binding energies. This emphasizes the important role of the partial local DOSs even quite far from the Fermi level for understanding the local chemical reactivity of a metal surface.

Finally we want to come back to the discrepancy between theory and experiment for the clean Rh(100) surface. Our calculations confirm those calculations of the surface electronic structure [31, 32] predicting non-magnetic surfaces. This prediction is not affected by using the GGA. Hence surface magnetism does not explain the discrepancy. On the other hand, we find that Rh and Pd behave in a very similar way and show strong adsorbate-induced outward relaxations. We suggest that the possible influence of contaminates is experimentally re-examined. Current work extends the *ab initio* investigations of the adsorption process on Rh and Pd to diatomic molecules (H_2, CO, ...).

Acknowledgment

This work was supported by the Austrian Science Foundation under project No P11353-PHY.

References

[1] Madix R J 1993 *Surface Reactions* (Berlin: Springer)
[2] Christmann K 1988 *Surf. Sci. Rep.* **9** 1
[3] Hamann D R and Feibelman P J 1988 *Phys. Rev.* B **37** 3847
[4] Feibelman P J and Hamann D R 1990 *Surf. Sci.* **234** 377
[5] Feibelman P J 1991 *Phys. Rev. Lett.* **67** 461
[6] Feibelman P J 1991 *Phys. Rev.* B **43** 9452
[7] Methfessel M, Hennig D and Scheffler M 1992 *Phys. Rev.* B **46** 4816
[8] Wilke S, Hennig D and Löber R 1993 *Surf. Sci.* **287+288** 89
[9] Wilke S, Hennig D and Löber R 1994 *Phys. Rev.* B **50** 2548
[10] Hammer B, Scheffler M, Jacobsen K W and Norskov J N 1994 *Phys. Rev. Lett.* **73** 1404
[11] White J A, Bird D M, Payne M C and Stich I 1994 *Phys. Rev. Lett.* **73** 1401
[12] Hammer B and Scheffler M 1994 *Phys. Rev. Lett.* **74** 3487
[13] Car R and Parrinello M 1985 *Phys. Rev. Lett.* **55** 2471
[14] Teter M P, Payne M C and Allan D C 1989 *Phys. Rev.* B **40** 12 255
[15] Payne M C, Teter M P, Allan D C, Arias T A and Joannopoulos J D 1992 *Rev. Mod. Phys.* **64** 1045
[16] Vanderbilt D 1990 *Phys. Rev.* B **41** 7892
[17] Kresse G and Hafner J 1994 *J. Phys.: Condens. Matter* **6** 8245
[18] Laasonen K, Pasquarello M, Car R, Lee C and Vanderbilt D 1991 *Phys. Rev.* B **47** 4174
[19] Kresse G and Hafner J 1994 *Phys. Rev.* B **48** 13 115
[20] Kresse G and Hafner J 1994 *Phys. Rev.* B **49** 14 251
[21] Kresse G and Furthmüller J 1996 *Comput. Mater. Sci.* at press
[22] Eichler A, Hafner J, Furthmüller J and Kresse G 1996 *Surf. Sci.* **346** 300
[23] Oed W, Dötsch B, Hammer L, Heinz K and Müller K 1988 *Surf. Sci.* **207** 55
[24] Hengrasmee S, Mitchell K A R, Watson P R and White J S 1980 *Can. J. Phys.* **58** 200
[25] Shepherd F R, Watson P R, Frost D C and Mitchell K A R 1980 *J. Phys. C: Solid State Phys.* **11** 4591
[26] Mitchell K A R, Shepherd F R, Watson P R and Frost D C 1977 *Surf. Sci.* **64** 737
[27] Watson P R, Shepherd F R, Frost D C and Mitchell K A R 1977 *Surf. Sci.* **72** 562
[28] Frost D C, Hengrasmee S, Mitchell K A R, Shepherd F R and Watson P R 1978 *Surf. Sci.* **76** L585
[29] Begley A M, Kim S K, Jona F and Marcus P M 1993 *Phys. Rev.* B **48** 12 326
[30] Morrison I, Bylander D M and Kleinman L 1993 *Phys. Rev. Lett.* **71** 1083
[31] Weinert M, Blügel S and Johnson P D 1993 *Phys. Rev. Lett.* **71** 4097
[32] Cho Jun-Hyung and Kang Myung-Ho 1995 *Phys. Rev.* B **52** 13 805
[33] Wu S C, Garrison K, Begley A M, Jona F and Johnson P D 1991 *Phys. Rev.* B **49** 14 081
[34] Kohn W and Sham L J 1965 *Phys. Rev.* **140** A1133

[35] Mermin N D 1965 *Phys. Rev.* **140** 1141
[36] Perdew J P and Zunger A 1981 *Phys. Rev.* B **23** 5048
[37] Becke A D 1988 *Phys. Rev.* A **38** 3098
[38] Perdew J P, Chevary J A, Vosko S H, Jackson K A, Pederson M R, Singh D J and Fiolhais C 1992 *Phys. Rev.* B **46** 6671
[39] von Barth U and Hedin L 1972 *J. Phys. C: Solid State Phys.* **5** 1629
[40] Louie S G, Froyen S and Cohen M L 1982 *Phys. Rev.* B **26** 1738
[41] Wood D M and Zunger A 1985 *J. Phys. A: Math. Gen.* **18** 1343
[42] Pulay P 1980 *Chem. Phys. Lett.* **73** 7892
[43] Perdew J P 1986 *Phys. Rev.* B **33** 8822
[44] Perdew J P and Wang Y 1986 *Phys. Rev.* B **33** 8800
[45] Kresse G, Furthmüller J and Hafner J 1994 *Phys. Rev.* B **50** 13 181
[46] Seifert K, Hafner J, Furthmüller J and Kresse G 1995 *J. Phys.: Condens. Matter* **6** 3683
[47] Villars P and Calvert L D 1985 *Pearson's Handbook of Crystallographic Data for Intermetallic Phases* (Metals Park, OH: American Society for Metals)
[48] Walker E, Ashkenazi J and Dacorogna M 1981 *Phys. Rev.* B **24** 2254
[49] Kittel C 1968 *Introduction to Solid State Physics* 3rd edn (New York: Wiley)
[50] Monkhorst H J and Pack J D 1976 *Phys. Rev.* B **13** 5188
[51] Methfessel M and Paxton A 1989 *Phys. Rev.* B **40** 3616
[52] Huber K P and Herzberg G 1979 *Constants of Diatomic Molecules (Molecular Structure and Molecular Spectra IV)* (New York: Van Nostrand-Reinhold)
[53] Hamann D R and Feibelman P J 1983 *Phys. Rev.* B **28** 3092
[54] Peebles D E, Peebles H C and White J M 1984 *Surf. Sci.* **136** 463
[55] Polizzotti R S and Ehrlich G 1979 *J. Chem. Phys.* **71** 259
[56] Richter L J and Ho W 1986 *J. Vac. Sci. Technol.* A **5** 453
[57] Richter L J, Germer T A, Sethna J P and Ho W 1988 *Phys. Rev.* B **38** 10 403
[58] Feibelman P J and Hamann D 1984 *Phys. Rev. Lett.* **52** 61
[59] Yang W and Parr R G 1985 *Proc. Natl Acad. Sci. USA* **82** 6723
[60] Harris J and Anderson S 1985 *Phys. Rev. Lett.* **55** 1583
[61] Hoffmann R 1988 *Rev. Mod. Phys.* **60** 601
[62] Cohen M H, Ganduglia-Pirovano M V and Kudrnovsky J 1994 *J. Chem. Phys.* **101** 3222
[63] Hammer B and Norskov J K 1995 *Surf. Sci.* **343** 211
[64] Behm R J, Christmann K and Ertl G 1980 *Surf. Sci.* **99** 320
[65] Besenbacher F, Stensgaard I and Mortensen K 1987 *Surf. Sci.* **191** 288
[66] Franken P E C, Bouwman R, Nieuwenhuys B E and Sachtler W H M 1974 *Thin Solid Films* **20** 243
[67] Tomanek D, Sun Z and Louie S G 1991 *Phys. Rev.* B **43** 4699
[68] Rayne T 1960 *Phys. Rev.* **118** 1545